Staphylococcal toxin induced preferential and prolonged *in vivo* deletion of innate-like B lymphocytes

Carl S. Goodyear and Gregg J. Silverman*

Rheumatic Disease Core Center, Department of Medicine, University of California at San Diego, La Jolla, CA 92093-0663

Communicated by J. Edwin Seegmiller, University of California at San Diego, La Jolla, CA, June 18, 2004 (received for review May 20, 2002)

Contributing to host defenses from the adaptive immune system, splenic marginal zone (MZ) B cells, with their preactivated state and special topographical location, serve essential roles as primary defenders from blood-borne microbes. From studies designed to define the immunologic impact of protein A of *Staphylococcus aureus* (SpA), a virulence factor with targeted B cell antigen receptor-binding properties, we found that within minutes of *in vivo* exposure, SpA became surface associated with B lymphocytes and induced trafficking. Within several hours, MZ were completely effaced of affected B cells. This was rapidly followed by massive B cell apoptosis, with accelerated preferential deletion of targeted MZ B cells and impaired responsiveness to T independent immunogens. Subsequently, the temporal recovery of MZ B cells was significantly delayed compared to peripheral follicular B cells (B-2 cells). These studies elucidate the cellular program induced by a natural toxin that is shown to be highly efficient at depleting innate-like B cells important for defense from systemic infection.

Blood-borne pathogens first encounter the adaptive immune system in the marginal zone (MZ) of the spleen, where a specialized population of B lymphocytes is perched outside of arteriolar marginal sinuses for unimpeded access. The major set of these MZ B cells display characteristic signaling profiles and a surface phenotype of memory B cells and express a distinct antigen (Ag)-binding repertoire (1). Although nonactivated MZ B cells are sessile (2), when their B cell receptors (BCR) bind Ag during thymic-independent (TI) responses, or after endotoxin or immune complex exposures, these B cells are reported to migrate out of the MZ and toward the T zones of the spleen (3–6). This controlled migration occurs following a gradient of chemokine levels and under the influence of neighboring macrophage populations (7) and changes in surface integrin molecules (8). These B cells are rapidly recruited into TI responses to complement-modified repetitive nonprotein determinants of infectious pathogens (9, 10), displaying a capacity for rapid clonal expansion and differentiation to Ag-specific Ab production, which provides a critical line of defense for invaders that have entered the bloodstream.

Different functional roles have been associated with recirculating peripheral follicular B cells (B-2 cells), the predominant set of mature splenic B cells. These lymphocytes, bearing a distinct surface phenotype and ligand signaling responsiveness, are recruited into T dependent responses after protein Ag immunization. Moreover, primary antiprotein responses follow slower kinetics but generally yield enhanced amnestic responses that do not commonly arise with TI responses. These separate mature B cell subsets offer an evolved tiered defense from the panoply of infectious threats.

The coevolution of common microbial pathogens with the adaptive immune system has led to a myriad of virulence strategies believed to enable manipulation and/or evasion of host defenses. To subvert the immune system, some microbes produce highly refined proteins, termed super-Ags (SAgs) due to their capacity for specific interactions, at high frequency, with lymphocyte Ag receptors, even without prior immune exposure. Most clinical isolates of *Staphylococcus aureus*, a common cause of life-threatening hematogenously spread infections, produce protein A of *S. aureus* (SpA). Although conventional Ag-specific lymphocytes are present in a naïve host at ≈1:1–10,000, SpA, has been termed a SAg for B cells, because 30–50% of human and ≈5–10% of murine B cells display Fab-mediated SpA-binding activity due to BCR framework interactions with clan V_HIII gene products (11–13). This V_H-binding specificity enables SpA to target supraclonal sets for BCR-mediated activation-associated apoptotic death that is T cell independent (14, 15), and deletion progresses to completion over ≈96 h (16). Although recent murine infection studies suggest that SpA acts as a virulence factor (17), the potential effects on host defenses are poorly understood.

To understand the impact of SpA on the immune system, we posed the questions whether all types of B cells bearing the targeted V_H regions are equally susceptible to this B cell SAg and how such induced imbalances in the composition of B cell pools may affect immune responsiveness. In the current studies, we have examined the functional and cellular implications of *in vivo* SpA exposure and found differential effects on distinct lymphoid subsets. Moreover, the impact of limited exposure on splenic populations was found to persist for many months, in part reflecting the host's varying capacity to heal supraclonal defects in different B cell compartments.

Methods

Mice. Studies were performed in C57BL/6 mice from The Jackson Laboratory and T15i transgenic "knockin" (18), which were bred and raised under specific pathogen-free conditions under the supervision of the University of California at San Diego Animal Subjects Program.

Flow Cytometry Analysis. Mononuclear cells were stained in the presence of Fc block as appropriate, adapting previously reported methods (12, 19), but included the specific mAbs for CD9 (clone KMC6) and CD11c and Gr-1 (BD Pharmingen). Data were acquired with a FACSCalibur (Becton Dickinson) and analyzed with FLOWJO software (Tree Star, Ashland, OR). Forward- and side-scatter gates included only nucleated viable cells; dead cells were excluded based on light scatter and/or 7-amino-actinomycin D uptake.

Ags, Treatments, and Immunizations. To track the *in vivo* distribution of cells that bind SpA, aliquots of recombinant SpA (rSpA) (Repligen) or ovalbumin (Sigma) were chemically conjugated to Alexa488-*N*-hydroxyl succimide (Molecular Probes), and groups of adult T15i mice then received 1 mg i.p. of labeled proteins. To

Abbreviations: Ag, antigen; BCR, B cell receptor; MZ, marginal zone; SAg, super-Ag; SpA, protein A of *Staphylococcus aureus*; TI, thymic independent; TNP, 2,4,6-trinitrophenyl; B-2, peripheral follicular B cells; T1, type 1.

*To whom correspondence should be addressed. E-mail: gsilverman@ucsd.edu.

www.pnas.org/cgi/doi/10.1073/pnas.0404382101

assess the impact on immune responsiveness, beginning within 24 h of birth, mice were treated with either saline alone, hen-egg lysozyme (HEL) (Sigma), or rSpA (Repligen). These neonatal mice received 100 μg of protein in PBS i.p. every other day for the first 2 wk of life (8×100 μg of protein), as reported (12, 14). Adult mice instead received a single i.p. dose of 1 mg of HEL or rSpA. Alternatively, doses were given on days 0 and 4, with harvest on day 6 (14, 15). Immunogens were purified to remove endotoxin and later tested by Limulus Amoebocyte assay, as described (15). Groups of mice were killed after different intervals, with harvest for immediate *ex vivo* analysis.

To evaluate the capacity to make specific TI Ab responses, different groups were treated with SpA or control protein as neonates, and 6 wk later mice were i.p. immunized with 50 μg of either 2,4,6-trinitrophenyl (TNP)-ficoll conjugates (Biosearch) or TNP-LPS (Biosearch) emulsified in complete Freund's adjuvant. Ab responses were assessed by comparisons of plasma obtained before and 2 wk after primary immunization. In all experiments, mice were age- and sex-matched.

Immunoassays of Ab Responses. To quantify the induced hapten-specific Ab response, microtiter wells were coated overnight with TNP-ovalbumin (Biosearch) at 5 μg/ml in PBS. After blocking with 2% BSA-PBS, serum samples, collected 14 days after immunization, diluted in block, and incubated on wells for 4 h at room temperature. The amount of bound Ab was determined by incubation with horseradish peroxidase (HRP)-labeled affinity-purified goat $F(ab')_2$ anti-mouse IgM- or IgG-specific reagent (Jackson ImmunoResearch). To measure the TNP-specific Abs that also display Fab-mediated binding interactions with SpA, we detected responses with a biotinylated form of chemically modified SpA devoid of Fcγ binding capacity (11), with subsequent development with HRP-labeled streptavidin (13). For quantitation, plates included a calibration curve of a purified TNP Ab-positive control sample to enable interpolation of Ab-binding reactivity to relative activity units.

Immunohistochemical Analyses. Adapting previously reported methods (15) to assess the distribution of affected B cells, frozen sections were stained either with biotinylated Abs or those directly labeled for the tags of fluorescein, rhodamine/Cy3 for immunofluorescence detection. B220 expression, which is not affected by SpA exposure, identified B cells (15), antimurine CD3-rhodamine identified T cells. To identify macrophage subsets and define the marginal sinus, follicular (B cell-rich) and extrafollicular/T cell-rich areas sections were costained with the macrophage receptor with collagenous structure (MARCO) or MOMA-1 mAbs (20) that identify marginal zone metallophilic macrophages.

Statistical Analysis. Comparisons between groups used the two-tailed Student *t* test.

Results

Preferential SpA-Binding Interactions with Defined Subsets of Splenic B Cells. We first evaluated the Fab-mediated SpA-binding capacity of defined B cell subsets from naïve adult C57BL/6 mice and T15i Ig "knockin" mice, which express a "knockin" clan V_HIII/S107 tg-encoded V_H region that mediates high-affinity SpA-binding interactions (14, 15, 18). Compared to C57BL/6 mice in which 6.8 ± 1.5% (mean ± SD, $n = 7$) of splenocytes bear the diagnostic B220$^+$ CD21^{hi} CD23^{lo} phenotype of the dominant MZ B cell set, there is a relative expansion of these splenic MZ B cells (29.7 ± 5.2%, $n = 7$) in naïve adult T15i$^{+/+}$ mice (Fig. 1 *A* and *C*).

From studies of the *in vitro* Fab-mediated SpA-binding capacity, we found that among the B cell precursors, the type 1 (T1) (B220$^+$CD24^{hi}CD21^{lo}) and type 2 (T2) (B220$^+$CD23^{hi}CD21^{hi}) transitional B cells (21), and the mature B cell sets, MZ B cells (B220$^+$CD21^{hi}CD23^{lo}), and follicular (B-2 cells) (B220$^+$CD21^{lo}CD23^{hi}), there was a clear hierarchy in the representation of strong SpA-binding activity (T2 > MZ > B-2 ≥ T1) in both C57BL/6 (Fig. 1*A*) and T15i$^{+/+}$ mice (Fig. 1*C*). However, levels of surface Igκ expression alone were inadequate to explain these differences in SpA-binding activity. In parallel studies of C57BL/6 mice, splenic B220$^+$CD1^{hi} B cells, a set largely overlapping with MZ (22) [and a smaller set representing T2 B cells (23)] also displayed a greater representation of higher SpA binders than did B220$^+$CD1^{lo} B cells, and this was also not solely due to surface Ig levels (not shown), suggesting that it likely reflects differences in expressed V_H repertoires. Similarly, splenic CD9^{hi} B cells, which primarily represent MZ B cells (24), also displayed a greater representation of strong SpA binders (Fig. 1 *B* and *D* and Fig. 7*A*, which is published as supporting information on the PNAS web site). Hence, we documented a bias for SpA-binding activity within the MZ B cell set, whereas there was a relative paucity of SpA binders in the conventional B-2 set.

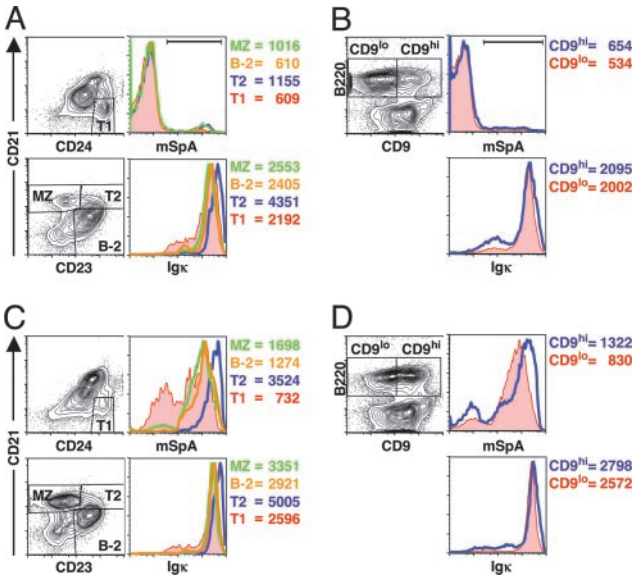

Fig. 1. Preferential *in vitro* SpA binding by defined subsets of naïve adult splenic B cells. In studies of adult C57BL/6 (*A* and *B*) and T15i$^{+/+}$ mice (*C* and *D*), after gating on B220$^+$ mononuclear cells, the B cell precursors, transitional B cell T1 and T2, and the mature B cell sets, MZ B cells and conventional B cells (B-2) were identified as indicated (*A* and *C*). The binding characteristics of CD9^{hi} B cells and CD9^{lo} B cells (*B* and *D*) are also displayed. The histograms and mean fluorescence intensity (MFI) for surface Igκ expression for these B cell sets are also shown. By use of a modified form of SpA (mSpA), the histograms for Fab-mediated SpA-binding activity for these defined subsets is shown. MFI values for mSpA binding of the T15i B cell subset or the C57BL/6 B cell subset under the horizontal bar are also indicated (representative of three independent experiments).

SpA Is Rapidly Bound *in Vivo* to B Cells That Undergo Induced Trafficking. We next investigated the *in vivo* distribution of fluorochrome-labeled SpA after i.p. administration. Despite the *in vivo* great molar excess of circulating Ig and capacity for infused SpA to form soluble immune complexes (25), we found that SpA became associated with B cells in diverse lymphoid sites within minutes after administration (Fig. 2). In the lymph nodes (LN) of T15i$^{+/+}$ mice, by 15 min after treatment, >80% of B cells bound high levels of labeled SpA. Significantly, compared to control-treated mice at this time point, there was a concurrent ≈30% depletion of B cells in LN (Fig. 2). In the bloodstream, the

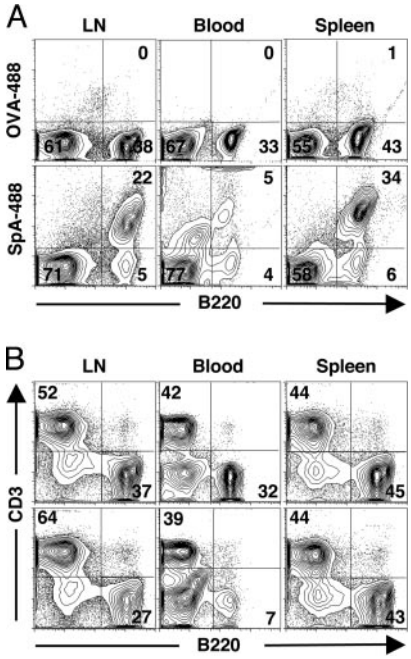

Fig. 2. After administration, labeled SpA rapidly becomes associated with B cells throughout the peripheral immune system. Adult T15i$^{+/+}$ mice received i.p. doses of Alexa-488 fluorochrome labeled SpA (SpA-488, *Lower*) or ovalbumin (OVA-488, *Upper*), and direct *ex vivo* binding levels with mononuclear cells were subsequently assessed, with representative studies from 15 min after treatment. (*A*) Based on B220 costaining, specific *in vivo* binding interactions with B cells after treatment with labeled SpA are demonstrated. (*B*) Based on B cell-to-T cell ratios, SpA treatment was shown to induce rapid depletion of the overall representation of B cells in the lymph nodes and blood but not in the spleen.

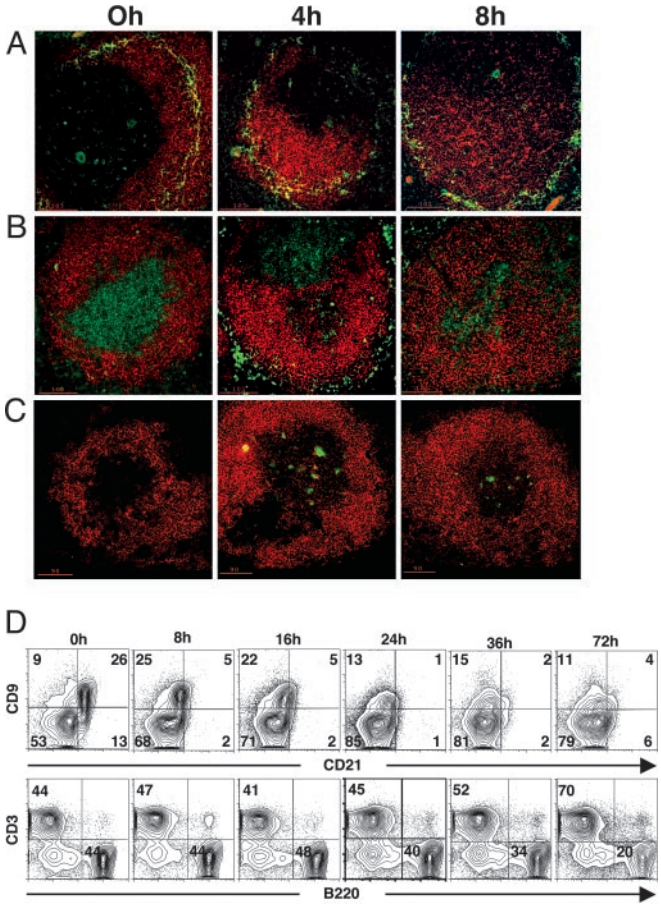

Fig. 3. SpA induces early effacement of B cells in the MZ and perferential loss of splenic CD9^{hi} T15i$^{+/+}$ B cells. Migration of B cells out of the MZ and into the follicle and T cell zones is shown in immunohistologic studies of T15i$^{+/+}$ splenic sections after control or SpA treatment, as indicated. Sections were stained for B220 in red and MOMA-1 in green (*A*), stained for B220 in red and CD3 in green (*B*), or stained for B220 in red and TUNEL in green (*C*). (*D*) From flow cytometric analysis, after gating on B220^{+} cells, costaining studies demonstrate that SpA treatment causes transient down-regulation of CD21 expression but does not affect CD9 expression. Dramatic progressive loss of CD9^{hi} B cells begins at 24 h after SpA treatment. (*Lower*) Based on B cell-to-T cell ratios, progressive overall B cell depletion is documented from 24 to 72 h after SpA treatment (representative of three independent experiments).

strongest flow cytometric signals for SpA interactions were also with T15i$^{+/+}$ B cells. In addition, we found that, at 15 min, there was an even greater depletion (i.e., ≈80%) of B cells from the bloodstream (Fig. 2). In the spleen, we again found that >90% of the cells associated with labeled SpA expressed B cell markers (Fig. 2*A*). In contrast, equivalent treatment of T15$^{+/-}$ and C57BL/6 mice demonstrated that labeled SpA binding was primarily associated with the transgene-expressing B cells (IgM^{a}) and a minority (≤15%) of endogenous B cells (Fig. 7 *B* and *C*). Significantly, whereas at these very early time points there was a distinct subset of T15i B cells that bound SpA, by 4 h, labeled SpA was associated with virtually all V_H-targeted T15i B cells (not shown). In these mice, we failed to detect B cell escape due to either induced V_H gene replacement or expression of endogenous V_H genes (not shown).

Unlike the rapid B cell depletion in the lymph nodes and bloodstream, during the first ≈16 h after SpA infusion, there was an initial enrichment of T15i$^{+/+}$ B cells in the spleen (15) (Fig. 2*B*), suggesting that during the early phases, the affected B cells traffic out of other peripheral sites and into the spleen. Consistent with these findings, we found deposition of labeled SpA on B220^{+} cells in primary follicles (not shown). In the blood but not at other sites, we also found weaker flow cytometric signals for labeled SpA associated with neutrophil granulocytes and CD11c$^{lo/intermed}$ immature dendritic cells (data not shown), which are reported to efficiently capture and transport whole particulate bacteria to the spleen (26).

SpA Induces Rapid Effacement of B Cells from the MZ. From histologic surveys, we found that by 4 h after SpA treatment, there was a rapid loss of T15i$^{+/+}$ B cells from the MZ, with a concurrent increase in the size of B cell follicles (Fig. 3 *A* and *B*). Moreover, by 8 h, the MZ was completely effaced of B cells and remained depleted at later time points (Fig. 3*A*) (data not shown), whereas the distribution of macrophage populations in the MZ, identified by MOMA-1 or MARCO, were not grossly affected (not shown). These findings are consistent with a recent report that BCR engagement can release MZ B cells from their integrin-mediated local retention, with migration toward the T cell-rich zones (8).

However, in contrast to productive immune responses, beginning at 4 h after SpA treatment, there were B220^{+} cells in or adjacent to the T cell zones that were also terminal deoxynucleotidyltransferase-mediated dUTP nick-end labeling-positive, a marker for apoptotic death (Fig. 3*C*), and bromodeoxyuridine labeling studies failed to detect induced proliferation in the spleen (not shown). This massive increase in the frequency of B cell apoptotic bodies peaked at ≈48 h after exposure, and by 96 h appeared to normalize (ref. 15 and Fig. 8, which is published as supporting information on the PNAS web site, and not shown), indicating the deletional process was complete.

SpA Induces Early Deletion of CD9^{hi} Splenic B Cells. To better quantify the effects on splenic B cell populations, flow cytomet-

ric studies were performed by using the $CD9^{hi}B220^{+}$ phenotype of MZ B cells, which we found was not affected by SpA interactions (Fig. 3*D* and ref. 15). These studies confirmed that the proportion of B cells in the spleen increased to peak at ≈16 h after treatment (15) (Fig. 3*D*) when the net entry of B cells appeared to ebb, when we also found that the representation of splenic $CD9^{hi}$ B cells was modestly decreased compared to baseline, presumably due in part to dilution from the induced entry of recirculating B-2 cells. However, by 24 h, a drop in the absolute number of B cells was documented, and there was an even greater preferential loss of affected $CD9^{hi}$ B cells (Fig. 3*D*). This decrease in the absolute number of splenic B cells and a greater decrease in the proportion of $CD9^{hi}$ B cells continued through ≈72 h after SpA treatment (Fig. 3*D*). In a representative study, at 72 h we found an overall mean loss of ≈73% of all $B220^{+}$ $T15i^{+/+}$ lymphocytes. Significantly, examination of defined B cell subsets documented a preferential ≈92% loss of the absolute number of $CD9^{hi}$ T15i splenic B cells, compared to ≈63% loss of the $CD9^{lo}$ splenic B cells that are predominantly B-2 cells (Fig. 3*D*). Moreover, we found no concurrent increase in $CD9^{hi}$ B cells in other lymphoid organs after SpA treatment (not shown). These findings, therefore, confirm histologic evidence that SpA induces a more rapid and preferential deletion of absolute number of MZ B cells compared to B-2 cells.

SpA Exposure Results in Long-Term MZ B Cell Depletion. To evaluate the long-term effects on V_H-targeted MZ B cells, studies were performed in hemizygotic $T15i^{+/-}$ mice, in which ≈30% of splenic B cells express the T15 V_H transgene marked by the IgM^a allotype, whereas the remainder use diverse endogenous V_H genes (and the IgM^b allotype) due to a breach in allelic exclusion (18). We found that 4 mo after SpA treatment of $T15i^{+/-}$ mice (for groups of three), there persisted a much greater depletion of IgM^a-expressing (SpA-susceptible) cells in the MZ compartment (51% mean depletion) compared to the B-2 compartment (40% mean depletion) (Fig. 4*A*). These findings were also confirmed in immunohistologic surveys (Fig. 9, which is published as supporting information on the PNAS web site). Hence, in $T15i^{+/-}$ mice long after SpA treatment, we also documented a persistent greater loss of high-affinity SAg-reactive IgM^a-bearing B cells from the MZ B cell compartment compared to B-2 cells.

To assess the effects of SpA treatment in mice that have polyclonal B cell populations, we determined the absolute number of splenic B cells that display Fab-mediated SpA-binding activity in each of these subsets in C57BL/6 mice. We found that in naïve or control-treated mice, there were $3.5 \pm 0.7 \times 10^6$ (mean ± SD) splenic MZ B cells with Fab-mediated SpA-binding capacity (Fig. 4*B*). Although SpA treatment did not alter the detectable overall representation of the distinct sets of splenic mature and precursor B cells (not shown), by 1 wk after SpA treatment, when the phenotype of residual B cells had recovered, there was a great decrease in the number of MZ B cells with SAg-binding capacity to $0.69 \pm 0.32 \times 10^6$, representing an ≈80% reduction compared to naïve or control-treated mice. Moreover, at progressively longer intervals after treatment, we documented a slow but progressive increase in this set of MZ B cells in the SpA-treated mice. However, even 18 wk after SpA treatment, there were only $2.0 \pm 0.79 \times 10^6$ SAg-reactive MZ B cells, representing a persistent ≈43% reduction in the absolute numbers of SAg-reactive MZ B cells. These studies suggest that after SpA treatment of C57BL/6 mice, the representation of these polyclonal SAg-reactive MZ B cells slowly normalized with a $t_{1/2}$ of ≈21 wk, as estimated by linear regression analysis. In parallel, although we found that naïve and control-treated C57BL/6 mice had $1.7 \pm 0.42 \times 10^6$ splenic B-2 cells with SAg-binding capacity, when evaluated 1 wk after SpA treatment, there were only $0.76 \pm 0.17 \times 10^6$ of these splenocytes

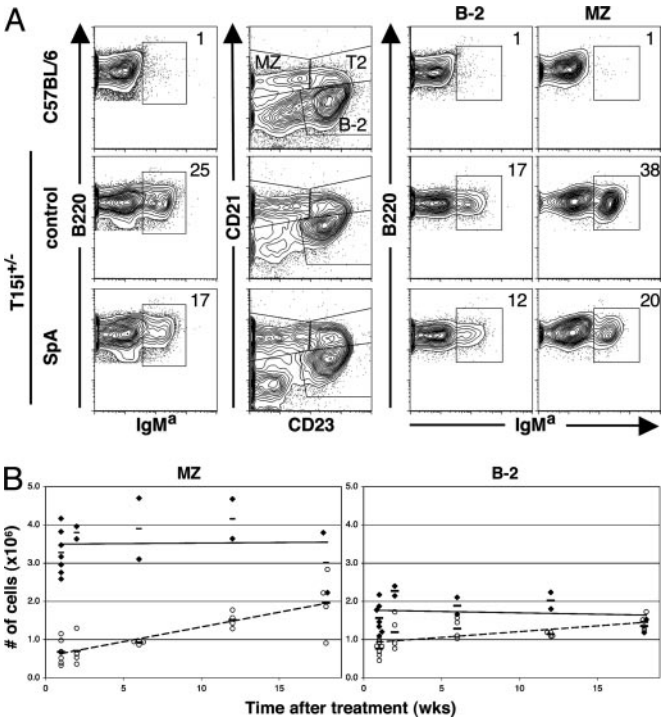

Fig. 4. Differential kinetics for recovery of SAg-reactive C57BL/6 splenic MZ and follicular B cells (B-2). (*A*) SpA results in loss of V_H susceptible B cells from the MZ of $T15i^{+/-}$ mice. Flow cytometric analyses were performed on splenic mononuclear cell suspensions of a control C57BL/6 or $T15i^{+/-}$ mice 4 mo after control or SpA treatment. After gating on $B220^{+}$ cells, splenic B cell subpopulations are identified based on the indicated CD21 and CD23 gates. (*B*) Age-matched groups of C57BL/6 mice received SpA or control treatment, and after different intervals mice were killed and flow cytometric analysis performed to assess the representation of B cells capable of Fab-mediated SpA-binding activity. B cell subsets were identified for MZ and B-2 cells, based on gating indicated in Fig. 1. Values are presented for the absolute number of each type of splenic cells with detectable Fab-mediated SpA-binding activity in individual mice after control treatment (◆) or SpA treatment (○). Data are compiled from studies of each time point, for which groups of two control- and four SpA-treated mice were evaluated in the same study. Studies were performed at time points when treatment-associated B cell phenotypic changes have normalized (not shown).

(Fig. 4*B*), indicating a mean ≈55% reduction. However, at subsequent time points, we documented a more rapid recovery of SAg-reactive B-2 cells, because by 18 wks the SpA-treated mice displayed $1.5 \pm 0.19 \times 10^6$ SAg-reactive splenic B-2 cells (≈12% reduction), the representation of B-2 cells recovered with a $t_{1/2}$ of ≈ 13 wk, which was a more rapid recovery than for the MZ B cell compartment.

SpA Treatment Results in Long-Term Defects in Thymus-Independent Ab Response. To investigate the functional implications of SpA exposure, groups of adult C57BL/6 mice were challenged with forms of TNP conjugated to carriers that impart TI responses that have been used to assess MZ immune functionality (9, 27). For groups of mice that had previously received either SpA or control treatment, after immunization with TNP coupled to LPS, a TI-1 conjugate, we found that both groups displayed a significant induction of IgM Abs specific for TNP, although there was a modest nonsignificant relative reduction of the postimmune IgM anti-TNP in the SpA-treated mice (Fig. 5*A*). In contrast, from assays that detect only the proportion of TNP-specific Abs reactive with the Fab-binding site of SpA, whereas control-treated mice had a significant induction of SAg-reactive anti-TNP Abs ($P = 0.03$), in the SpA-treated group there was no

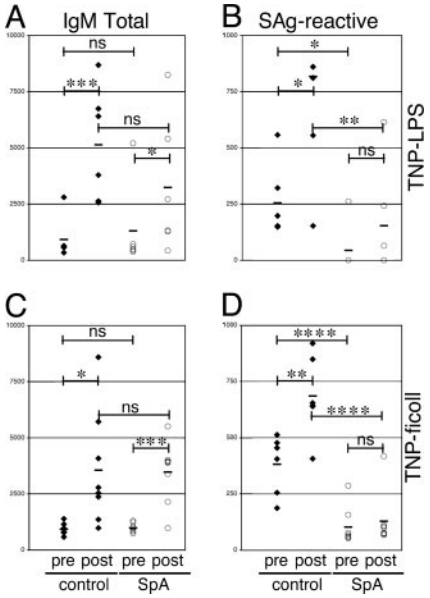

Fig. 5. SpA treatment results in functional impairment of TI anti-TNP Ab responses from V_H-targeted B cells. Groups of age-matched C57BL/6 mice received control or SpA treatment and after 2 weeks received immunizations with either TNP-LPS (TI-1) (*A* and *B*) or TNP-ficoll (TI-2) (*C* and *D*) immunogens. Two weeks after immunization, Ab responses were evaluated based on detection with tagged anti-IgM reagent (*A* and *C*) or tagged mSpA (*B* and *D*), which detects Fab-mediated SpA binding reactivity (12). Values in relative units were derived by interpolation from a standard curve of an IgM anti-TNP control. Pre- and postimmune anti-TNP values from individual mice are displayed after control (◆) or SpA treatment (○). Each group contained six or eight mice, as indicated. Statistical significance was determined for pre- and postimmune responses of a group based on the two-tailed paired Student *t* test, whereas other comparisons used the unpaired *t* test. *P* values are represented by *, <0.05; **, <0.01; ***, < 0.005; and ****, <0.005.

significant induction of SAg-reactive anti-TNP Abs (Fig. 5*B*). Hence, we found a significant impairment of the pre- and postimmunization anti-TNP responses derived from the B cells targeted by SpA ($P < 0.01$).

The same pattern of selectively impaired Ab responses was also found with the TI-2 immunogen, TNP-ficoll. Both treatment groups displayed significant inductions of IgM anti-TNP responses, because SpA did not affect overall IgM anti-TNP responses (Fig. 5*C*). However, although the control-treated group had an induction of postimmune SAg-reactive anti-TNP responses ($P < 0.01$), there was no significant induction of anti-TNP Abs from SpA-targeted B cells in mice with prior exposure to SpA ($P = 0.0001$) (Fig. 5*D*). Hence, consistent with evidence of the targeted loss of these mature B cells, we found that SpA treatment also induced a concurrent loss of functional responsiveness to an immunogen that has been shown to require a functional MZ compartment (27).

Discussion

The current studies demonstrate that exposure to SpA can induce a long-lasting V_H-targeted supraclonal defect in the *in vivo* representation and functional responsiveness of MZ B cells. Within hours of SpA treatment, there was a massive migration of B cells out of the MZ with the concurrent expansion of the follicle. Moreover, the effacement of B cells from the MZ occurred without the appearance of these lymphocytes in other peripheral lymphoid tissue, indicating that this was not due to egress. Our finding of preferential deletion after an *in vivo* encounter with this BCR-targeted microbial toxin is consistent with evidence that MZ B cells have lower BCR-negative signaling thresholds (1). In mice expressing endogenous V_H genes, the proportion of MZ B cells with *in vitro* and *in vivo* binding capacity for SpA was reproducible, greater than for follicular B cells (Figs. 1 and 7), presumably due to differences in repertoire. Taken together, our studies suggest that the V_H-targeted deletion of B cells occurs in sequential or overlapping waves, with the deletion of MZ B cells occurring more quickly and more efficiently than for conventional follicular B cells.

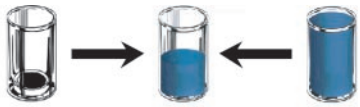

	Rate of healing ($t_{1/2}$)	Rate of decay ($t_{1/2}$)
Recirculating Follicular B cells (B-2)	13 weeks	18 weeks
Marginal Zone B cells	21 weeks	$\rightarrow \infty$
B-1 cells	$\rightarrow \infty$	$\rightarrow \infty$

Fig. 6. Rates of healing and decay of MZ B cells. Rates of healing were derived from a linear regression analysis, by using EXCEL (Microsoft), of the current studies of SAg treatment and recovery of B-2 and MZ B cells in C57BL/6 mice and from our reported studies in B-1 cells (14). Rates of decay were from Hao and Rajewsky (29).

Most cell-associated labeled SpA was bound *in vivo* to V_H-targeted B cells. However, akin to the recent report that neutrophil granulocytes and $CD11c^{lo/intermed}$ immature dendritic cells can mediate transport of *S. pneumoniae* bacteria (26), we also found that labeled SpA was associated with these cells in the blood, although this was not the predominant association in the spleen. In addition, although bacterial interactions with MARCO scavenger receptor on a subset of MZ macrophages have been reported to be central to the subsequent induced migration of MZ B cells (7), SpA treatment did not induce a redistribution of splenic macrophages.

Our studies are distinct from previously described B cell ablative approaches to measure the rate of refilling of peripheral compartments (reviewed in ref. 28), because SpA does not completely empty the peripheral B cell pools but instead causes a targeted V_H-restricted B cell deletion. Hence, we assessed the healing/recovery of defined supraclonal B cell sets when peripheral B cell compartments have not been entirely emptied. Our studies document that after SAg-induced deletion the clonal diversity within the mature B cell pools in the spleen can be healed, although this induced immunologic defect persisted long after central B lymphogenesis resumed the export of B cell precursors. Specifically, we found that the B-2 cell pool in C57BL/6 mice normalized with a $t_{1/2}$ of ≈13 wk, whereas the selective immunodefect in the polyclonal MZ pool recovered much more slowly after SpA treatment (i.e., $t_{1/2} \approx 21$ wk). A comparable pattern was also demonstrated in $T15i^{+/-}$ mice, but here the induced deficits resolved even more slowly, presumably due to the greater deletion of the T15 V_H-expressing B cells that have among the highest binding affinity for SpA (13). Furthermore, B cell SAg exposure also resulted in a prolonged selective immunodefect in TI responses of C57BL/6 mice.

Our studies provide a perspective on B cell turnover that is complementary to the recent report in which the conditional regulation of RAG-2 was used to turn off the somatic assembly of Ig and T cell receptor V genes and block central lymphocyte development (29). From this system, in which mature pools could no longer be replenished, peripheral follicular B cells (i.e., B-2 cells) were shown to decay with an estimated $t_{1/2}$ of ≈18 weeks. In contrast, these studies also demonstrated that levels of splenic MZ B cells and peritoneal B-1 cells remained at near normal levels throughout the period of observation. Hence, our

studies of SAg challenge and subsequent lymphoid healing have provided a validating counterpoint to studies of the turnover of mature B cell pools previously obtained from a genetic approach to estimate compartment-specific cellular decay rates (Fig. 6).

MZ B and B-1 cells have been described as tiers of "innate-like B lymphocytes" that play critical roles in the defense from many infectious agents (30–32). We found that SpA induced a V_H-targeted defect in immune responsiveness to experimental TI-1 and TI-2 immunogens, which confirmed a linked induced functional defect. These findings extend our earlier evidence that SpA induced a V_H-targeted defect in the B-1 cell pool that appeared to be permanent. In the current studies, we found that targeted MZ B cells are also highly susceptible to SpA, and this induced defect was more severe, persistent, and slower to heal than for B-2 cells. Moreover, because replenishment into the MZ B cell set may occur from immature B cells (33), as well as memory B cells from germinal centers (5, 34) or recirculating B cells (9, 35, 36), our studies provide a perspective on compartmental recovery rates that could not otherwise be accurately measured by bromodeoxyuridine labeling studies. In retrospect, the persistent loss of MZ B cells induced by SpA may also have contributed to our earlier finding that SpA exposure can induce immunologic tolerance to phosphoryl choline (PC) (14), because it was subsequently reported that B cell clones within the MZ and B-1 compartment work together in anti-PC immune responses (32). Hence, it now seems that the PC-specific immunologic tolerance induced by SpA is due to the deletion of both V_HIII-encoded MZ and B-1 cell responses.

SpA has been shown to act as a virulence factor contributing to increased mortality (17). Our studies demonstrate that upon entry into the circulation, this bacterial toxin directly associates with the membrane Ig of targeted B cells leading to a redistribution in lymphoid sites that may immunocompromise the host. Hence, the functional properties of this bacterial toxin appear well suited to thwart, or even provide a preemptive attack on, the preformed defenses of the "innate-like" B cell pools. We speculate that clones in the B-1 and/or MZ B cell pools can recognize and respond to staphylococcal determinants, representing essential contributors to host defenses. In fact, because the V_HIII clan is highly conserved among mammalian species (16), this postulated virulence strategy may have preceded the appearance of mice and humans. Moreover, a convergent strategy may also have been adopted by *Peptococcus magnus*, which produces a Fab-binding protein that targets a conserved germline V_L framework site, conveying the same preferential MZ B cell targeting and capacity to induce V_κ-targeted apoptotic death (19) by pathways recently demonstrated for SpA.

Conclusion

As localization and control of an infection may be determined by whether the host can mobilize immune defenses before the pathogen proliferates and spreads, we speculate that toxins such as SpA may at times provide an advantage to the infectious invader. Immunization with a nonprotein staphylococcal component has been shown to induce protective immune responses, whereas immunization with whole bacteria could not (37). We wonder, therefore, whether the above-described B cell-active mechanisms may impair the host's ability to develop a protective immune response following staphylococcal infection.

We thank Drs. John Kearney and Flavius Martin for suggestions and critical review of the manuscript. We acknowledge the help of the University of California at San Diego Cancer Center Histology and Immunohistology Core and James Feramisco and the Cancer Center Digital Imaging Core. This work was supported by Grants AI40305, AR47360, AR50659, and AI46637 from the National Institutes of Health and the Alliance for Lupus Research (to G.J.S.) and Grant CA104815 from the National Institutes of Health, the Cancer Research Institute, and the National Blood Foundation (to C.S.G.).

1. Oliver, A. M., Martin, F., Gartland, G. L., Carter, R. H. & Kearney, J. F. (1997) *Eur. J. Immunol.* **27,** 2366–2374.
2. Gray, D., MacLennan, I. C., Bazin, H. & Khan, M. (1982) *Eur. J. Immunol.* **12,** 564–569.
3. Gray, D., Kumararatne, D. S., Lortan, J., Khan, M. & MacLennan, I. C. (1984) *Immunology* **52,** 659–669.
4. Groeneveld, P. H., Erich, T. & Kraal, G. (1985) *Immunobiology* **170**, 402–411.
5. Liu, Y. J., Oldfield, S. & MacLennan, I. C. (1988) *Eur. J. Immunol.* **18,** 355–362.
6. Vinuesa, C. G., Sunners, Y., Pongracz, J., Ball, J., Toellner, K. M., Taylor, D., MacLennan, I. C. & Cook, M. C. (2001) *Eur. J. Immunol.* **31,** 1340–1350.
7. Karlsson, M. C., Guinamard, R., Bolland, S., Sankala, M., Steinman, R. M. & Ravetch, J. V. (2003) *J. Exp. Med.* **198,** 333–340.
8. Lu, T. T. & Cyster, J. G. (2002) *Science* **297,** 409–412.
9. Lane, P. J., Gray, D., Oldfield, S. & MacLennan, I. C. (1986) *Eur. J. Immunol.* **16,** 1569–1575.
10. Oliver, A. M., Martin, F. & Kearney, J. F. (1999) *J. Immunol.* **162,** 7198–7207.
11. Silverman, G. J., Sasano, M. & Wormsley, S. B. (1993) *J. Immunol.* **151,** 5840–5855.
12. Silverman, G. J., Nayak, J. V., Warnatz, K., Cary, S., Tighe, H. & Curtiss, V. E. (1998) *J. Immunol.* **161,** 5720–5732.
13. Cary, S., Krishnan, M., Marion, T. N. & Silverman, G. J. (1999) *Mol. Immunol.* **36,** 769–776.
14. Silverman, G. J., Cary, S. P., Dwyer, D. C., Luo, L., Wagenknecht, R. & Curtiss, V. E. A. (2000) *J. Exp. Med.* **192**, 87–98.
15. Goodyear, C. S. & Silverman, G. J. (2003) *J. Exp. Med.* **197,** 1125–1139.
16. Cary, S. P., Lee, J., Wagenknecht, R. & Silverman, G. J. (2000) *J. Immunol.* **164,** 4730–4741.
17. Palmqvist, N., Foster, T., Tarkowski, A. & Josefsson, E. (2002) *Microb. Pathog.* **33,** 239–249.
18. Taki, S., Meiering, M. & Rajewsky, K. (1993) *Science* **262,** 1268–1271.
19. Goodyear, C., Narita, M. & Silverman, G. J. (2004) *J. Immunol.* **172,** 2870–2877.
20. Kraal, G. & Janse, M. (1986) *Immunology* **58,** 665–669.
21. Loder, F., Mutschler, B., Ray, R. J., Paige, C. J., Sideras, P., Torres, R., Lamers, M. C. & Carsetti, R. (1999) *J. Exp. Med.* **190,** 75–89.
22. Roark, J. H., Park, S. H., Jayawardena, J., Kavita, U., Shannon, M. & Bendelac, A. (1998) *J. Immunol.* **160,** 3121–1327.
23. Martin, F. & Kearney, J. F. (2002) *Nat. Rev. Immunol.* **2,** 323–335.
24. Won, W. J. & Kearney, J. F. (2002) *J. Immunol.* **168,** 5605–5611.
25. Das, C. & Langone, J. J. (1987) *Cancer Res.* **47,** 2002–2007.
26. Balazs, M., Martin, F., Zhou, T. & Kearney, J. (2002) *Immunity* **17,** 341–352.
27. Claassen, E., Kors, N. & Van Rooijen, N. (1986) *Eur. J. Immunol.* **16,** 492–497.
28. Fulcher, D. A. & Basten, A. (1997) *Immunol. Cell Biol.* **75,** 446–455.
29. Hao, Z. & Rajewsky, K. (2001) *J. Exp. Med.* **194,** 1151–1164.
30. Briles, D. E., Forman, C., Hudak, S. & Claflin, J. L. (1982) *J. Exp. Med.* **156,** 1177–1185.
31. Baumgarth, N., Herman, O. C., Jager, G. C., Brown, L. E., Herzenberg, L. A. & Chen, J. (2000) *J. Exp. Med.* **192,** 271–280.
32. Martin, F., Oliver, A. M. & Kearney, J. F. (2001) *Immunity* **14,** 617–629.
33. Martin, F. & Kearney, J. F. (2000) *Immunity* **12,** 39–49.
34. Dunn-Walters, D. K., Isaacson, P. G. & Spencer, J. (1995) *J. Exp. Med.* **182,** 559–566.
35. Dammers, P. M., de Boer, N. K., Deenen, G. J., Nieuwenhuis, P. & Kroese, F. G. (1999) *Eur. J. Immunol.* **29,** 1522–1531.
36. Vinuesa, C. G., Sze, D. M., Cook, M. C., Toellner, K. M., Klaus, G. G., Ball, J. & MacLennan, I. C. (2003) *Eur. J. Immunol.* **33,** 297–305.
37. McKenney, D., Pouliot, K. L., Wang, Y., Murthy, V., Ulrich, M., Doring, G., Lee, J. C., Goldmann, D. A. & Pier, G. B. (1999) *Science* **284,** 1523–1527.